Int J Adv Manuf Technol (2016) 86:1739–1751
DOI 10.1007/s00170-015-8314-5

ORIGINAL ARTICLE

Thermal error compensation of dry hobbing machine tool considering workpiece thermal deformation

Huajun Cao[1] · Libin Zhu[1] · Xianguang Li[2] · Peng Chen[2] · Yongpeng Chen[1]

Received: 2 October 2015 / Accepted: 28 December 2015 / Published online: 12 January 2016

Abstract Dry hobbing is a new gear tooth forming process, which would replace the traditional wet hobbing process due to its high efficiency and environmental friendliness. However, due to the absence of metal cutting fluid in dry hobbing, temperature of hobbed workpiece is relatively high, which will lead to the increase of dimension errors, especially tooth thickness errors. In this paper, the features of workpiece thermal deformation errors are identified and an error compensation model is developed to compensate both machine tool thermal errors and tooth thickness errors which is induced by workpiece thermal deformation. In this model, the representative temperature variables of a dry hobbing machine tool are obtained based on experimental data with fuzzy clustering method. A compensation model is proposed to map the relationship between representative temperature variables and compensation value. In a series of experiments, the tooth thickness errors ranged from −22 to −59 μm. After implementing compensation of machine tool thermal errors, the tooth thickness errors ranged from −18 to −28 μm, which demonstrates that workpiece thermal deformation has a great influence on tooth thickness errors in dry hobbing. Furtherly, the tooth thickness errors ranged from −4 to 8 μm, after implementing compensation of both machine tool thermal errors and workpiece thermal deformation errors, which demonstrate that the compensation model is effective.

✉ Huajun Cao
hjcao@cqu.edu.cn

[1] State Key Laboratory of Mechanical Transmission, Chongqing University, Chongqing 400044, China

[2] Chongqing Machine Tool (Group) Co., Ltd., Chongqing 400055, China

Keywords Thermal errors · Dry hobbing · Workpiece thermal deformation · Compensation model · Tooth thickness errors

1 Introduction

Gear hobbing is the leading manufacturing technology for mass production of gears, especially for automobile gears. Considering that an average number of 15 gears are hobbed per car [1], and 86 millions of cars were produced in 2014, gear hobbing produced 1290 millions automobile gears per year. That means gear hobbing is a large-scale industrial production activity. However, the widely used wet gear hobbing process, which consumes lots of metal cutting fluid, leads to the environmental pollution and healthy risk of workers. In recent years, dry hobbing process becomes available, and it would replace wet hobbing process in the coming future quickly, due to its high efficiency and environmental friendliness.

According to Bryan [2], thermal errors, which make up 40–70 % of the total machine tool errors, are the greatest contributors to machine tool errors. With continuous development of industry, the requirement for processing precision becomes higher. In recent years, researches on machine tool thermal errors are focus on precision machining [3–5]; however, few of them take workpiece thermal deformation into consideration when it refers to hobbing machine tool [6]. Because hobbing is a semi-finishing process, and in wet hobbing, good cooling and lubricating characteristics of metal cutting fluid makes the temperature variation of hobbed workpiece too little to affect workpiece accuracy. Whereas in dry hobbing, there are more friction and adhesion between hob and workpiece, which would increase the temperature variation of hobbed workpiece due to the absence of metal cutting fluid [7]. The increased temperature of workpiece usually enlarge

workpiece dimensional errors and tooth profile errors, especially for low width-radius ratio gear. In practical production of dry hobbing, unstable ambient temperature and machine tool state, which would lead to the bad consistency of temperature of hobbed workpiece, makes the tooth thickness of some hobbed workpiece cannot meet the design requirements.

There are generally three ways to reduce thermal errors: thermal error avoidance, thermal error control, and thermal error compensation [8]. Compared with thermal error avoidance and thermal error control, thermal error compensation technique is cost-effective relatively [9]. It is demonstrated that the machine tool thermal error compensation model could be established using experimental measurements with multiple regression analysis techniques [4, 10, 11], artificial neural networks [5, 12, 13], grey system theory [14], etc. This paper proposes a thermal error compensation model of dry hobbing machine tool, which is used for mass production of external gear, with consideration of workpiece thermal deformation. The compensation model is divided into two parts: workpiece thermal deformation error compensation model and machine tool thermal error compensation model. The relation between hobbed workpiece temperature and workpiece thermal deformation errors is analyzed. Then, representative temperature variables of a dry hobbing machine tool are obtained based on experimental data with fuzzy clustering method. The prediction model of hobbed workpiece temperature, as well as machine tool thermal error compensation model, is developed by multiple regression method. And, the workpiece thermal deformation error compensation model is obtained based on the prediction model of hobbed workpiece temperature. A series of experiments were carried out on the dry hobbing machine tool to evaluate the validity of the model. As a result, the tooth thickness errors ranged from −18 to −28 μm, after implementing compensation of machine tool thermal errors only. And, the tooth thickness errors ranged from −4 to 8 μm, after implementing compensation of both machine tool thermal errors and workpiece thermal deformation errors. The result shows that workpiece thermal deformation has a great influence on tooth thickness errors in dry hobbing, and the compensation model is effective.

2 Thermal errors of machine tool and workpiece

The errors, which affect the machining accuracy, can be divided into several groups as follows [15]:

(1) Geometric and kinematic errors;
(2) Thermal errors;
(3) Cutting-force induced errors;
(4) Errors induced by tool wear and errors induced by assembling and chattering [16, 17].

In wet machining, thermal errors, which make up 40–70 % of the total errors, are the largest contributor to the dimensional errors of a workpiece. In dry hobbing, the workpiece thermal deformation enlarges the dimensional errors of workpiece that caused by thermal deformation.

Due to the characteristics of hobbing, thermal errors in y and z directions are infinitesimal compared with thermal errors in x direction. So, thermal errors in x direction are analyzed in this paper. In this situation, the machining accuracy of hobbing machine tool is influenced by the accuracy of distance between centers of the hob spindle and workpiece spindle in x direction. Eddy current displacement sensor is mounted on the machine tool for measuring the variation of distance between centers of hob spindle and workpiece spindle in x direction, which is equal to the machine tool thermal errors in x direction.

In dry hobbing, the thermal deformation of workpiece lead to the variation of workpiece parameters. As shown in section 2.2, workpiece thermal deformation errors compensation, as well as machine tool thermal error compensation, can be realized by adding an extra movement to the hob spindle. So, the compensation value, δ, could be divided into two parts: machine tool thermal error compensation value, δ_M, and workpiece thermal error compensation value, δ_T.

2.1 Analysis of machine tool thermal errors

Temperature rise in a machine structure start from a few heat sources, which cause the uneven temperature distribution. The temperature gradient, which induced by the uneven temperature distribution, makes the components of machine tool, such as lathe bed and columns, deformed. It leads to the variation of the distance between centers of the hob spindle and workpiece spindle in x direction, which is equal to the machine tool thermal errors in x direction and the machine tool thermal error compensation value, δ_M, as shown in Fig. 1.

Empirical models have been demonstrated to show that it has a satisfactory prediction accuracy for application. Multiple regression method can be used to map the relationship between the thermal errors and temperature variables. The common method to choose locations of temperature sensors is to

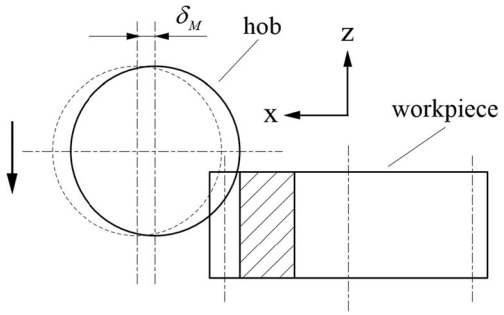

Fig. 1 Schematic diagram of compensation value of machine tool thermal errors

preset a large number of sensor locations. Then, the representative ones, which will be used in the final thermal error compensation model, can be chosen based on fuzzy clustering method. In this paper, machine tool thermal error compensation model is established based on multiple linear regression method, that is, δ_M can be expressed as follows:

$$\delta_M = a_0 + a_1 \Delta T_1 + \cdots + a_p \Delta T_p + \varepsilon \quad (1)$$

Where $\Delta T_1, \ \ldots, \ \Delta T_p$ are the temperature variation of the temperature variables, $a_0 \ , \ldots, \ a_p$ are regression coefficients, ε is called the residual, or noise.

The procedures of machine tool thermal error compensation are as follows. Firstly, the thermal error compensation model is established based on experimental data of machine tool thermal errors and thermal resistances' temperature and stored in SCM. Then, during machining process, the thermal error compensation model is used to calculate the compensation value in accordance with the temperature of representative thermal resistances. Finally, the compensation value is sent to the CNC of the machine tool, and an extra movement is added to the hob spindle to compensating thermal errors.

2.2 Analysis of workpiece thermal deformation errors

In dry hobbing, the thermal deformation of workpiece lead to the variation of workpiece parameters. The following parameters are mainly affected by workpiece thermal deformation: tooth profile, tip diameter, root diameter, face width, etc. The thermal deformation of tooth profile will deteriorate the machining precision of next process, shaving or grinding, if the tooth thickness cannot meet the design requirements. So, the purpose of compensating workpiece thermal deformation errors is to make sure that tooth thickness value of hobbed workpiece is larger than the minimum design requirements on the same Y-circle. That is, $\Delta s_y > 0$, as shown in Fig. 3.

In ordinary wet hobbing, the good cooling effect of metal cutting fluid makes the temperature of workpiece that just hobbed, T_a, close to the temperature of metal cutting fluid. While in dry hobbing, T_a is susceptible to ambient temperature and machining time due to the bad cooling condition, that is, the variation of T_a is in a large range. So, it is hard to control the parameters of workpiece when it is cooled to the design temperature, T_b. In order to realize the compensation of workpiece thermal deformation errors, the prediction model of T_a should be established. In this paper, setting 20 °C as the value of T_b.

$$\Delta T_w = T_a - T_b \quad (2)$$

According to the character of hobbing, temperature of points on the same cylinder of hobbed workpiece are approximatively equal. A series of experiments were taken to figure out the temperature field of hobbed workpiece. The experimental apparatus are shown in section 4. As shown in Fig. 2, temperature variation of points on the same cylinder of hobbed workpiece is less than 0.7 °C. It demonstrates that the temperature of hobbed workpiece is approximately symmetric. Table 1 shows the temperature of points from A1 to A17, the maximum difference of which is 1.6 °C. So, the temperature field of hobbed workpiece can be simplified down to even steady-state temperature field. The average value of those 17 points is defined as the value of T_a in this paper.

In order to figure out the relation between δ_T and workpiece thermal deformation errors, the variation of workpiece parameters that resulting from compensation and workpiece thermal deformation should be analyzed. Figure 3 shows the schematic diagram of gear in S_1, S_2, and S_3. Where S_1 is the design state, S_2 is the state that the workpiece is just hobbed with compensation, and S_3 is the state that the workpiece is cooled to T_b.

The compensation of workpiece thermal deformation errors makes the profile of hobbed workpiece shift from S_1 to S_2, as shown in Fig. 3. The profile shift coefficient, x, is found as

$$x = \frac{\delta_T}{m} \quad (3)$$

Hobbing process would not change the tip diameter of workpiece, d_{a3}, which means

$$d_{a3} = d_{a1} \quad (4)$$

The tip diameter of workpiece in S_2, d_{a2}, is found as

$$d_{a2} = (1 + \Delta T_w \lambda) d_{a1} \quad (5)$$

The tooth thickness half angle at Y-cylinder in S_1, ψ_{y1}, is found as

$$\psi_{y1} = \psi_1 + \mathrm{inv}\alpha - \mathrm{inv}\alpha_{y1} \quad (6)$$

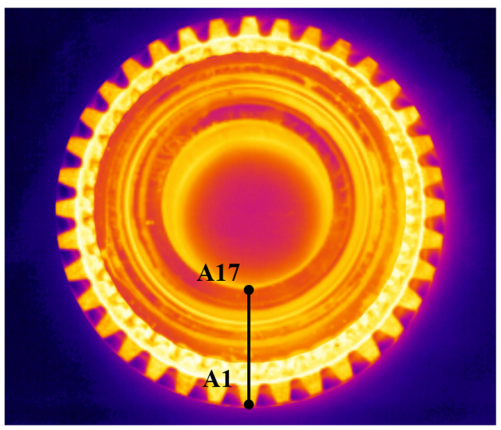

Fig. 2 Thermography of hobbed workpiece

Table 1 Temperature of points on hobbed workpiece

Number of points	A1	A2	A3	A4	A5	A6	A7	A8	A9
Temperature (°C)	61.1	61.3	61.0	61.1	61.4	61.7	61.5	61.1	60.7
Number of points	A10	A11	A12	A13	A14	A15	A16	A17	
Temperature (°C)	60.4	60.6	60.7	60.5	60.3	60.4	60.1	60.2	

The tooth thickness on the Y-cylinder of gear in S_1, s_{y1}, is produced by

$$s_{y1} = d_{y1}\psi_{y1} = d_{y1}\left[\psi_1 + \text{inv}\alpha - \text{inv}\alpha_{y1}\right] = d_{y1}\left[\frac{\pi}{2z} + \text{inv}\alpha - \text{invarccos}\left(\frac{r}{r_{y1}}\cos\alpha\right)\right] \quad (7)$$

The tooth thickness half angle of the reference circle of workpiece in S_2, ψ_2, is found as

$$\psi_2 = \frac{\pi}{2z} + \frac{2\tan\alpha}{mz}\delta_T \quad (8)$$

The tooth thickness on the Y-cylinder of workpiece in S_2, s_{y2}, is produced by

$$s_{y2} = d_{y2}\psi_{y2} = d_{y2}\left[\psi_2 + \text{inv}\alpha - \text{inv}\alpha_{y2}\right] = d_{y2}\left[\frac{\pi}{2z} + \frac{2\tan\alpha}{mz}\delta_T + \text{inv}\alpha - \text{invarccos}\left(\frac{r}{r_{y2}}\cos\alpha\right)\right] \quad (9)$$

Workpiece thermal deformation makes workpiece profile shift from S_2 to S_3, as shown in Fig. 3. For Y point on the tooth profile of workpiece in S_2, the position change, which result from workpiece thermal deformation, is divided into two directions: tooth thickness direction and radial direction. So, when workpiece is cooled to T_b, the diameter of Y-circle is produced by

$$d_{y3} = (1-\Delta T_w\lambda)d_{y2} \quad (10)$$

The variation of tooth thickness half angle of Y point is found as

$$\Delta\psi = \frac{\Delta T_w\lambda s_{y2}}{(1-\Delta T_w\lambda)d_{y2}} = \frac{\Delta T_w\lambda}{(1-\Delta T_w\lambda)}\psi_{y2} \quad (11)$$

Tooth thickness half angle at Y-cylinder of workpiece in S_3 is produced by

$$\psi_{y3} = \psi_{y2} - \Delta\psi = \frac{1-2\Delta T_w\lambda}{1-\Delta T_w\lambda}\psi_{y2} \quad (12)$$

Tooth thickness on the Y-cylinder of workpiece in S_3 is produced by

$$s_{y3} = d_{y3}\psi_{y3} = (1-\Delta T_w\lambda)d_{y2}\frac{1-2\Delta T_w\lambda}{1-\Delta T_w\lambda}\psi_{y2} = (1-2\Delta T_w\lambda)s_{y2} \quad (13)$$

On condition that $d_{y1} = d_{y3}$, the difference between s_{y3} and s_{y1}, Δs_y, is calculated using

$$\Delta s_y = s_{y3} - s_{y1} = (1-2\Delta T_w\lambda)d_{y2}\left[\frac{\pi}{2z} + \frac{2\tan\alpha}{mz}\delta_T + \text{inv}\alpha - \text{invarccos}\left(\frac{r}{r_{y2}}\cos\alpha\right)\right] - (1-\Delta T_w\lambda)d_{y2}\left[\frac{\pi}{2z} + \text{inv}\alpha - \text{invarccos}\left(\frac{r}{(1-\Delta T_w\lambda)r_{y2}}\cos\alpha\right)\right] \quad (14)$$

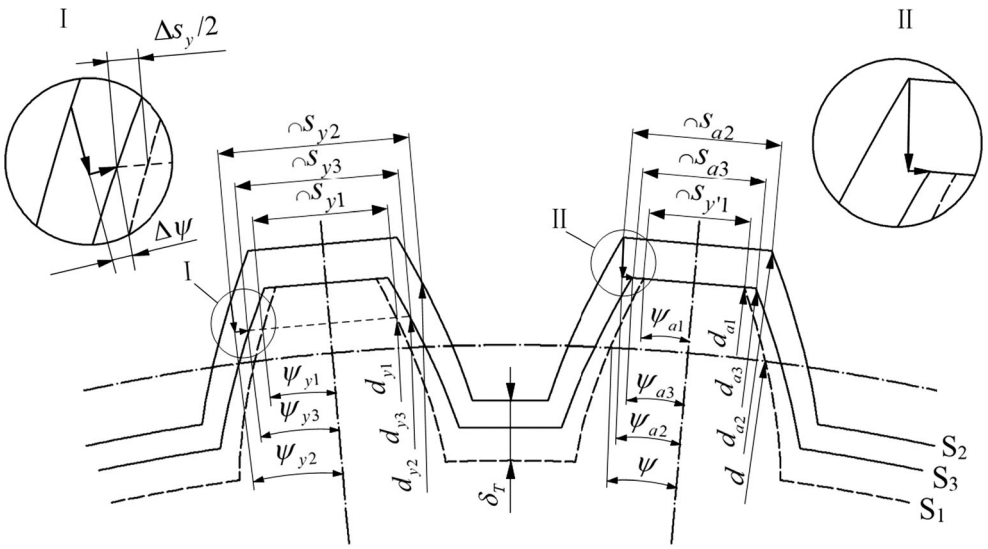

Fig. 3 Schematic diagram of workpiece in three states

In order to make sure that the machining allowance is qualified, the following condition should be satisfied:

$$\Delta s_y > 0 \tag{15}$$

According to Eq.(14), there is a positive correlation between Δs_y and d_{y2}, that means the following condition should be satisfied:

$$s_{a3} - s_{a1} = 0 \tag{16}$$

The crest width of gear in S_2, s_{a2}, is produced by

$$s_{a2} = d_{a2}\psi_{a2} = (1 + \Delta T_w \lambda) d_{a1} \left[\frac{\pi}{2z} + \frac{2\tan\alpha}{mz} \delta_T + \mathrm{inv}\alpha - \mathrm{invarccos}\left(\frac{r}{(1 + \Delta T_w \lambda) r_{a1}} \cos\alpha \right) \right] \tag{17}$$

The crest width of gear in S_3, s_{a3}, is produced by

$$\begin{aligned} s_{a3} &= (1 - 2\Delta T_w \lambda)\, s_{a2} \\ &= (1 - 2\Delta T_w \lambda)(1 + \Delta T_w \lambda) d_{a1} \left[\frac{\pi}{2z} + \frac{2\tan\alpha}{mz} \delta_T + \mathrm{inv}\alpha - \mathrm{invarccos}\left(\frac{r}{(1 + \Delta T_w \lambda) r_{a1}} \cos\alpha \right) \right] \end{aligned} \tag{18}$$

In S_1, tooth thickness on the Y-circle, whose diameter is d_{a2},, is produced by

$$s_{a1} = d_{a1}\psi_{a1} = d_{a1} \left[\frac{\pi}{2z} + \mathrm{inv}\alpha - \mathrm{invarccos}\left(\frac{r}{r_{a1}} \cos\alpha \right) \right] \tag{19}$$

δ_T can be calculated from Eq. (16), Eq. (18), and Eq. (19):

$$\delta_T = \frac{m}{2\tan\alpha} \left[\frac{\pi + 2z\mathrm{inv}\alpha - 2z\mathrm{invarccos}\left(\frac{r}{r_{a1}} \cos\alpha \right)}{2(1 - 2\Delta T_w \lambda)(1 + \Delta T_w \lambda)} - \frac{\pi}{2} - z\mathrm{inv}\alpha + z\mathrm{invarccos}\left(\frac{r}{(1 + \Delta T_w \lambda) r_{a1}} \cos\alpha \right) \right] \tag{20}$$

Equation (20) shows the relationship between δ_T and ΔT_w. According to Eq.(2) and Eq. (20), δ_T can be written as

$$\delta_T = F(T_a) \tag{21}$$

3 Experiments

Experiments were carried out on a YE3120CNC7 dry hobbing machine tool that manufactured by Chongqing Machine Tool Group Co Ltd. During machining, the hob spindle speed was set at 900 rpm. The external involute gear, whose module was 2.5 mm, was hobbed by one time feeding. Parameters of the hob and the workpiece are shown in Table 2.

Measuring instruments for experiments are as follows: Pt-100 thermal resistances, infrared camera, eddy current displacement sensor, data acquisition device, computer, Klingelnberg Gear Measuring Center, calculagraph, etc. Before experiments, thermal resistances and eddy current displacement sensor were calibrated in national authorized computation & attestation centers. And the material emissivity of workpiece, which would be used to set the parameter of infrared camera, was calibrated too. The data acquisition device was composed of National Instruments data acquisition system. The data acquisition software was programmed in LabVIEW. The following kinds of data were recorded during experiments: temperature of thermal resistances, displacement

Table 2 Parameters of hob and workpiece

Hob		
Heads: $K = 3$	Diameter: $D = 70$ mm	Aperture: $d = 32$ mm
Length: $L = 160$ mm		
Gear		
$m = 2.5$ mm	$z = 36$	
Reference pressure angle: $\alpha_f = 20°$		

Table 3 Locations of thermal resistances

Thermal resistance's number	Location of thermal resistances	Thermal resistance's number	Location of thermal resistances
T#1	Environment	*T*#8	Workpiece column
T#2	Machine bed	*T*#9	Inside space of machine tool
T#3	Anterior end cover of hob spindle	*T*#10	Inlet pipe of lube oil
T#4	Rear end cover of hob spindle	*T*#11	Outlet pipe of lube oil
T#5	Bearing end cover of hob spindle	*T*#12	Inlet pipe of hydraulic oil
T#6	Bearing end cover of hob shifting spindle	*T*#13	Outlet pipe of hydraulic oil
T#7	Bearing end cover of workpiece spindle	*T*#14	Workpiece clamping cylinder

variation value that measured with eddy current displacement sensor, temperature of hobbed workpiece that measured with infrared camera, tooth thickness of workpiece that measured with Klingelnberg Gear Measuring Center, NO. of hobbed workpiece, time, etc. As the machine tool need to be adjusted after test hobbing, the number of workpiece for test hobbing was not counted into the hobbed workpiece.

Veldhuis and Elbestawi [18] did some researches to find the optimal number of thermal resistances for five-axis machine tool. Mou [19] mounted 40 thermal resistances on the CNC machining center to estimate and correct time-varying machine tool errors with desired accuracy. In this paper, 14 Pt-100 thermal resistances were mounted on the dry hobbing machine tool. The locations of thermal resistances, which are shown in Table 3 and Fig. 4, are close to the main heat sources including:

(1) Cutting zone;
(2) Air cooling system;
(3) Hydraulic oil and lubricating oil;
(4) Motors;
(5) Bearings, guides;
(6) Drives and clutches;
(7) Rotary device of double worm gear and worm pair;
(8) Environment.

In those experiments, the dry hobbing machine tool kept running for about 4 h, until 145 workpieces were hobbed. The machine paused for 12 min after machining for 66 min. A series of experimental temperature data of thermal resistances are shown in Fig. 5. The ambient temperature, which ranged from 23.6 to 28 °C, is shown in Fig. 5a. Figure 5b–d show that the temperature of measurement points *T*#2-*T*#14 rise with fluctuation when machining. Figure 6 shows the thermal errors of the dry hobbing machine tool in *x* direction. The absolute variation value of machine tool thermal errors, which range from 0 to 29 μm, increase with the machining time. Figure 7 shows that the temperature of hobbed workpiece, T_a, which ranges from 53 to 68 °C, increase with the machining time. And, T_a become steady as the number of hobbed workpiece increasing.

4 Modeling

4.1 Modeling algorithm

The procedures of modeling are shown in Fig. 8. The number of temperature variables has a critical impact on the accuracy of the error compensation model. An excessive number will increase the amount of calculation and costs, and the interaction of various temperature variables will reduce the accuracy and robustness of the model. So, the temperature variables must be optimized before modeling. Fuzzy clustering method is used to dividing variables into some clusters. The similarity of temperature variables was described by similarity coefficient, $r_{TT\,ij}$, as shown in Eq. (23). Temperature variables were

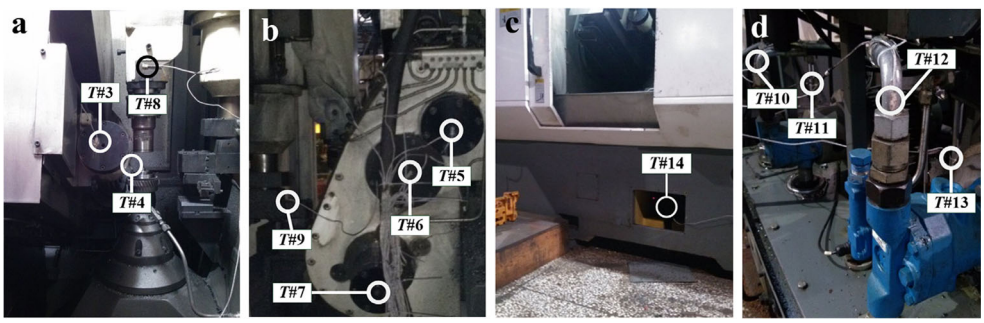

Fig. 4 Locations of thermal resistances. **a** *T*#3, *T*#4, *T*#8. **b** *T*#5, *T*#6, *T*#7, *T*#9. **c** *T*#14 **d** *T*#10, *T*#11, *T*#12, *T*#13

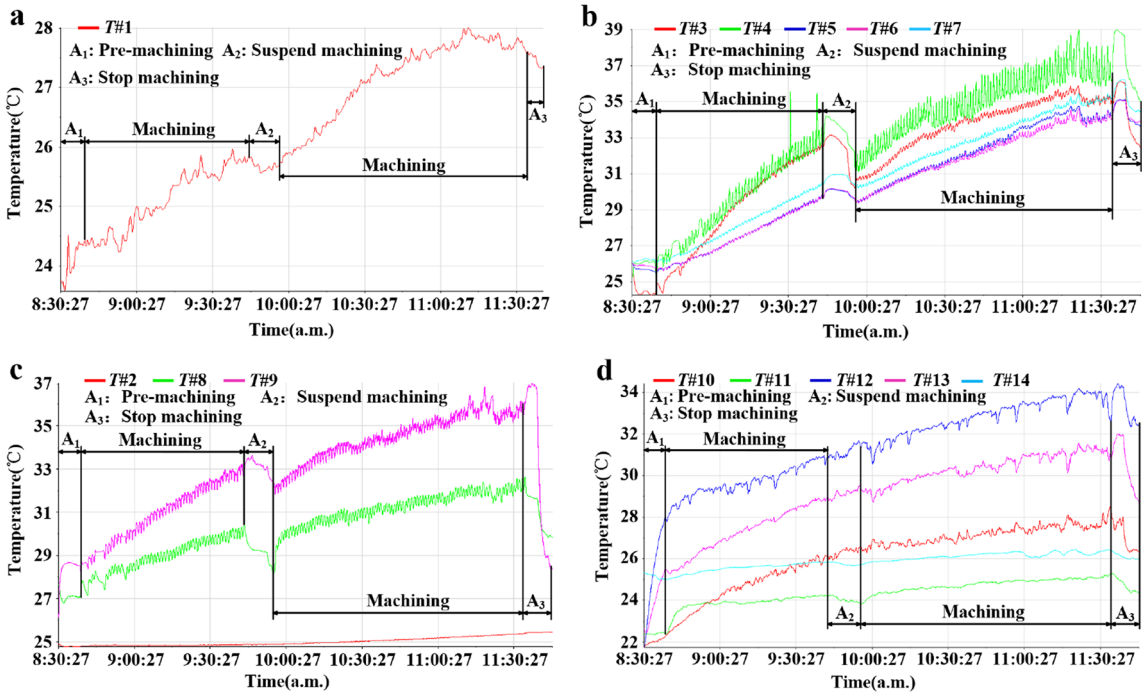

Fig. 5 Temperature of thermal resistances. **a** *T*#1. **b** *T*#3-*T*#7. **c** *T*#2, *T*#8, *T*#9. **d** *T*#10-*T*#14

classified into some clusters according to the similarity coefficient.

Then, a representative temperature variable is selected from each cluster according to its correlation with the machine tool thermal errors or workpiece temperature. In this paper, machine tool thermal errors model is established by multiple linear regression method. According to the researches of cutting temperature [20], the main factors that affect the cutting temperature are as follows:

(1) Material of cutting tool and workpiece;
(2) Cutting speed, feed speed, cutting depth, shear angle;
(3) Cutter rotation angle;
(4) Cooling condition.

On the condition that workpiece parameters and machining parameters are unchanged, the factors that influence T_a are cooling conditions, such as ambient temperature, cutting zone temperature, etc. So, in this paper, multiple linear regression method can be used to establish the prediction model of T_a, as well as machine tool thermal error compensation model. And, the prediction model of T_a is verified available in section 5. Workpiece thermal deformation error compensation model can be established with the prediction model of T_a and Eq. (21).

As the compensation of both machine tool thermal errors and workpiece deformation errors are realized by adding an extra movement to the tool spindle to change the distance between centers of hob spindle and workpiece spindle in x direction. The compensation value, δ, could be calculated by

$$\delta = \delta_M + \delta_T \tag{22}$$

4.2 Fuzzy clustering of temperature variables

The similarity of temperature variables is described by similarity coefficient, $r_{TT\ ij}$, which be used to estimate the

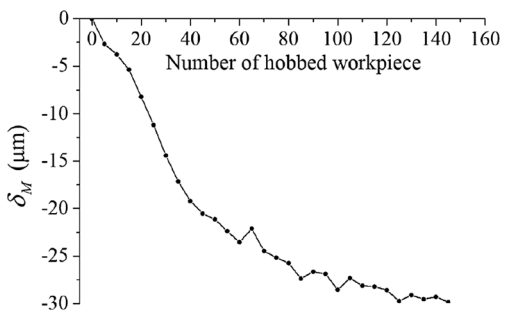

Fig. 6 Machine tool thermal errors in x direction

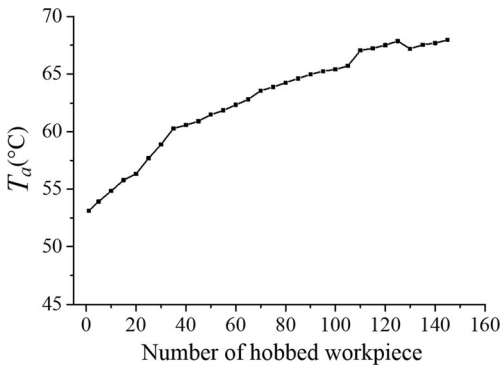

Fig. 7 Temperature of hobbed workpiece

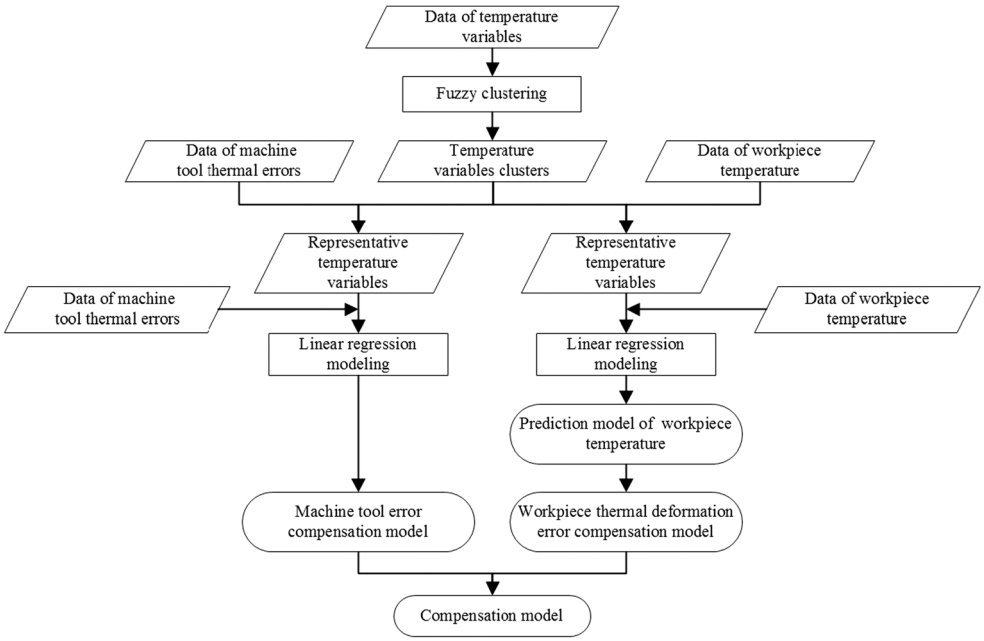

Fig. 8 Procedures of modeling

correlation between the temperature variables. In this paper, $r_{TT\ ij}$ is calculated by Eq. (23).

$$r_{TT\ ij} = \frac{\sum_{k=1}^{n}\left(T_{ik}-\overline{T}_i\right)\left(T_{jk}-\overline{T}_j\right)}{\sqrt{\sum_{k=1}^{n}\left(T_{ik}-\overline{T}_i\right)^2}\sqrt{\sum_{k=1}^{n}\left(T_{jk}-\overline{T}_j\right)^2}} \tag{23}$$

Where T_i ($i=1, \ldots, p$) is the temperature variable of $T\#i$ ($i=1, \ldots, p$), $\overline{T}_i = \frac{1}{n}\left(\sum_{k=1}^{n} T_{ik}\right)$, $\overline{T}_j = \frac{1}{n}\left(\sum_{k=1}^{n} T_{jk}\right)$

Table 4 shows the similarity matrix that is calculated from a set of data of temperature variables. Figure 9 shows the cluster tree of temperature variables.

A variety of clusters can be obtained from the tree diagram. According to the machine tool structure, those temperature variables are clustered to six clusters as follows: $\{T_5, T_6, T_7, T_9, T_{12}, T_{13}\}, \{T_{10}\}, \{T_3, T_4\}, \{T_8, T_{11}, T_{14}\}, \{T_1\}, \{T_2\}$.

4.3 Machine tool thermal error modeling

The correlation coefficient, $r_{T\delta m}$, which is used to estimate the correlation between temperature variables and thermal errors, is calculated using

Table 4 Similarity matrix of temperature variables

	T_1	T_2	T_3	T_4	T_5	T_6	T_7	T_8	T_9	T_{10}	T_{11}	T_{12}	T_{13}	T_{14}
T_1	1.000	0.904	0.891	0.905	0.951	0.953	0.951	0.915	0.937	0.923	0.947	0.965	0.944	0.950
T_2	0.904	1.000	0.852	0.871	0.951	0.943	0.941	0.913	0.906	0.839	0.950	0.935	0.878	0.916
T_3	0.891	0.852	1.000	0.972	0.958	0.961	0.964	0.918	0.980	0.935	0.898	0.921	0.949	0.923
T_4	0.905	0.871	0.972	1.000	0.965	0.971	0.970	0.896	0.981	0.940	0.901	0.934	0.952	0.920
T_5	0.951	0.951	0.958	0.965	1.000	0.999	0.999	0.945	0.987	0.954	0.958	0.983	0.973	0.957
T_6	0.953	0.943	0.961	0.971	0.999	1.000	1.000	0.942	0.990	0.960	0.954	0.983	0.978	0.958
T_7	0.951	0.941	0.964	0.970	0.999	1.000	1.000	0.940	0.990	0.961	0.950	0.983	0.979	0.957
T_8	0.915	0.913	0.918	0.896	0.945	0.942	0.940	1.000	0.946	0.895	0.971	0.931	0.918	0.953
T_9	0.937	0.906	0.980	0.981	0.987	0.990	0.990	0.946	1.000	0.957	0.938	0.963	0.972	0.951
T_{10}	0.923	0.839	0.935	0.940	0.954	0.960	0.961	0.895	0.957	1.000	0.886	0.947	0.976	0.921
T_{11}	0.947	0.950	0.898	0.901	0.958	0.954	0.950	0.971	0.938	0.886	1.000	0.950	0.919	0.968
T_{12}	0.965	0.935	0.921	0.934	0.983	0.983	0.983	0.931	0.963	0.947	0.950	1.000	0.981	0.952
T_{13}	0.944	0.878	0.949	0.952	0.973	0.978	0.979	0.918	0.972	0.976	0.919	0.981	1.000	0.935
T_{14}	0.950	0.916	0.923	0.920	0.957	0.958	0.957	0.953	0.951	0.921	0.968	0.952	0.935	1.000

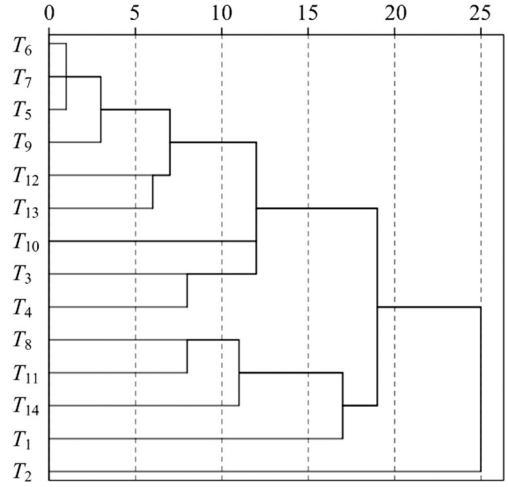

Fig. 9 Cluster tree of temperature variables

$$r_{T\delta m\ i} = \frac{\sum_{k=1}^{n}\left(T_{ik}-\overline{T}_i\right)\left(\delta_{M\ \ k}-\overline{\delta}_M\right)}{\sqrt{\sum_{k=1}^{n}\left(T_{ik}-\overline{T}_i\right)^2}\sqrt{\sum_{k=1}^{n}\left(\delta_{M\ \ k}-\overline{\delta}_M\right)^2}} \quad (24)$$

Where $\overline{T}_i = \frac{1}{n}\left(\sum_{k=1}^{n} T_{ik}\right)$, $\overline{\delta}_M = \frac{1}{n}\left(\sum_{k=1}^{n}\delta_{M\ \ k}\right)$

Table 5 shows the correlation coefficients which are calculated from the data of temperature variables and machine tool thermal errors. The temperature variable, whose correlation with the thermal errors is bigger than others in the cluster, is chosen from each cluster as the representative temperature variable. As a result, the representative temperature variables are T_1, T_2, T_4, T_{10}, T_{13}, T_{14}.

The general form of multiple regression analysis models is as follows:

$$\delta_M = a_0 + a_1\Delta T_1 + a_2\Delta T_2 + \cdots + a_p\Delta T_p + \varepsilon \quad (25)$$

The multiple linear regression model of δ_M can be calculated as follows:

$$\begin{cases} \boldsymbol{\delta} = \Delta\boldsymbol{T}\boldsymbol{A} + \boldsymbol{\varepsilon} \\ \boldsymbol{\varepsilon} \sim \boldsymbol{N}_n\left(0, \sigma^2\boldsymbol{I}_n\right) \end{cases} \quad (26)$$

Where $\boldsymbol{I}_n$ is the identity matrix;

$$\boldsymbol{A}_{7\ 1} = [a_0\ \ a_1\ \ \cdots\ \ a_6]^{\mathrm{T}},\quad \boldsymbol{\delta}_n = [\delta_{M0}\ \ \delta_{M1}\ \ \cdots\ \ \delta_{Mn}]^{\mathrm{T}},\quad \boldsymbol{\varepsilon}_n = [\varepsilon_0\ \ \varepsilon_1\ \ \cdots\ \ \varepsilon_n]^{\mathrm{T}};$$

$$\Delta\boldsymbol{T}_{n\ 7} = \begin{bmatrix} 1 & \Delta T_{1\ 1} & \cdots & \Delta T_{1\ 13} & \Delta T_{1\ 14} \\ 1 & \Delta T_{2\ 1} & \cdots & \Delta T_{2\ 13} & \Delta T_{2\ 14} \\ \vdots & \vdots & \ddots & \vdots & \vdots \\ 1 & \Delta T_{n\ 1} & \cdots & \Delta T_{n\ 13} & \Delta T_{n\ 14} \end{bmatrix}.$$

The least-square estimation of $\boldsymbol{A}_{7\ 1}$ makes residual sum of squares $S_E^2(\boldsymbol{A})$ to a minimum, that is,

$$\begin{cases} \hat{\boldsymbol{\delta}}_{n\ 1} = \Delta\hat{\boldsymbol{T}}_{n\ 7}\cdot\hat{\boldsymbol{A}}_{7\ 1} \\ \dfrac{\partial}{\partial\boldsymbol{A}}\mathrm{S}_{\mathrm{E}}^2\left(\hat{\boldsymbol{A}}\right) = 0 \end{cases} \quad (27)$$

Where $\hat{\boldsymbol{A}}_{7\ 1} = [\hat{a}_0\ \ \hat{a}_1\ \ \cdots\ \ \hat{a}_6]^{\mathrm{T}}$ is the estimator of $\boldsymbol{A}$. In conclusion, $\hat{\boldsymbol{A}}_{7\ 1}$ can be calculated using

$$\hat{\boldsymbol{A}}_{7\ 1} = \left(\Delta\hat{\boldsymbol{T}}_{n\ 7}^{\mathrm{T}}\Delta\hat{\boldsymbol{T}}_{n\ 7}\right)^{-1}\Delta\hat{\boldsymbol{T}}_{n\ 7}^{\mathrm{T}}\hat{\boldsymbol{\delta}}_{n\ 1} \quad (28)$$

$\hat{\boldsymbol{A}}_{7\ 1}$ can be obtained by substituting experimental data of representative temperature variables into Eq. (28), the result is

$$\hat{\boldsymbol{A}}_{7\ 1} = [-0.90, -1.18, -7.12, -0.03, -1.94, -0.26, 2.43]^{\mathrm{T}} \quad (29)$$

So, δ_M can be expressed as follows:

$$\begin{aligned} \delta_M =&\ \mathrm{H}\ \ (\Delta T_1, \Delta T_2, \Delta T_4, \Delta T_{10}, \Delta T_{13}, \Delta T_{14}) \\ =&\ -0.90 - 1.18\Delta T_1 - 7.12\Delta T_2 - 0.03\Delta T_4 - 1.94\Delta T_{10} - 0.26\Delta T_{13} \\ &+ 2.43\Delta T_{14} \end{aligned} \quad (30)$$

4.4 Workpiece thermal deformation error modeling

Similarly, the similarity coefficient, r_{TTa}, which is used to estimate the correlation between temperature variables and T_a, is calculated using

Table 5 Correlation coefficient between thermal resistance temperature and machine tool thermal errors variables

	T_1	T_2	T_3	T_4	T_5	T_6	T_7	T_8	T_9	T_{10}	T_{11}	T_{12}	T_{13}	T_{14}
$r_{T\delta m}$	0.956	0.862	0.903	0.948	0.958	0.963	0.962	0.818	0.946	0.990	0.864	0.961	0.983	0.908

Table 6 Correlation coefficient between thermal resistance temperature and hobbed workpiece temperature variables

	T_1	T_2	T_3	T_4	T_5	T_6	T_7	T_8	T_9	T_{10}	T_{11}	T_{12}	T_{13}	T_{14}
r_{TTa}	0.987	0.923	0.952	0.976	0.990	0.992	0.991	0.891	0.982	0.969	0.936	0.982	0.985	0.963

$$r_{TTa\,i} = \frac{\sum_{k=1}^{n}\left(T_{ik}-\overline{T}_i\right)\left(T_{ak}-\overline{T}_a\right)}{\sqrt{\sum_{k=1}^{n}\left(T_{ik}-\overline{T}_i\right)^2}\sqrt{\sum_{k=1}^{n}\left(T_{a\ k}-\overline{T}_a\right)^2}} \tag{31}$$

Where $\overline{T}_i = \frac{1}{n}\left(\sum_{k=1}^{n} T_{ik}\right)$, $\overline{T}_a = \frac{1}{n}\left(\sum_{k=1}^{n} T_{a\ k}\right)$

Table 6 shows the correlation coefficient that was calculated from the data of temperature variables and hobbed workpiece temperature, T_a. The temperature variable, whose correlation with the hobbed workpiece temperature is bigger than others in the cluster, is chosen from each cluster as the representative temperature variable. As a result, the representative temperature variables are T_1, T_2, T_4, T_6, T_{10}, T_{14}.

The machining accuracy is usually adjusted before machining. Thus, it is the variation of temperature that affect machine tool thermal errors, that is, ΔT_1, ΔT_2, ΔT_4, ΔT_{10}, ΔT_{13}, ΔT_{14} could be used to establish the machine tool thermal error compensation model. While in modeling of T_a, the temperature of hobbed workpiece is influenced by the initial temperature of environment and machine tool components, so temperature of hobbed workpiece are expressed with the following temperature variables: T_1, T_2, T_4, T_6, T_{10}, T_{14}. That is, T_a can be expressed as follows:

$$T_a = b_0 + b_1T_1 + b_2T_2 + \cdots + b_pT_p + \varepsilon \tag{32}$$

The prediction model of T_a can be calculated as follows:

$$\begin{cases} \boldsymbol{T}_a = \boldsymbol{TB} + \boldsymbol{\varepsilon} \\ \boldsymbol{\varepsilon} \sim \boldsymbol{N}_n\left(0, \sigma^2\boldsymbol{I}_n\right) \end{cases} \tag{33}$$

Where $\boldsymbol{I}_n$ is the identity matrix;

$$\boldsymbol{B}_{7\ 1} = [b_0 \quad b_1 \quad \cdots \quad b_6]^{\mathrm{T}},\ \boldsymbol{T}_{a\ n} = [T_{a\ 0} \quad T_{a\ 1} \quad \cdots \quad T_{a\ n}]^{\mathrm{T}},\ \boldsymbol{\varepsilon}_n = [\varepsilon_0 \quad \varepsilon_1 \quad \cdots \quad \varepsilon_n];$$

$$\boldsymbol{T}_{n\ 7} = \begin{bmatrix} 1 & T_{1\ 1} & \cdots & T_{1\ 10} & T_{1\ 14} \\ 1 & T_{2\ 1} & \cdots & T_{2\ 10} & T_{2\ 14} \\ \vdots & \vdots & \ddots & \vdots & \vdots \\ 1 & T_{n\ 1} & \cdots & T_{n\ 10} & T_{n\ 14} \end{bmatrix};$$

The least-square estimation of $\boldsymbol{B}_{7\ 1}$ makes residual sum of squares $S_E^2(\boldsymbol{B})$ to a minimum, that is,

$$\begin{cases} \hat{\boldsymbol{T}}_{an\quad 1} = \hat{\boldsymbol{T}}_{n\ 7}\cdot\hat{\boldsymbol{B}}_{7\quad 1} \\ \frac{\partial}{\partial \boldsymbol{B}} \mathrm{S}_{\mathrm{E}}^2\left(\hat{\boldsymbol{B}}\right) = 0 \end{cases} \tag{34}$$

Where $\hat{\boldsymbol{B}}_{7\ 1} = [b_0 \ \ b_1 \ \ \cdots \ \ b_6]^{\mathrm{T}}$ is the estimator of $\boldsymbol{B}$.

In conclusion, $\hat{\boldsymbol{B}}_{7\ 1}$ can be calculated using

$$\hat{\boldsymbol{B}}_{7\ 1} = \left(\hat{\boldsymbol{T}}_{n\ 7}^{\mathrm{T}}\hat{\boldsymbol{T}}_{n\ 7}\right)^{-1}\hat{\boldsymbol{T}}_{n\ 7}^{\mathrm{T}}\hat{\boldsymbol{T}}_{a\ n\ 1} \tag{35}$$

Substitute $\hat{\boldsymbol{T}}_{n\quad 7}$ and $\hat{\boldsymbol{T}}_{a\ n\quad 1}$ into Eq. (35), the result is

$$\hat{\boldsymbol{B}}_{7\ 1} = [56.80, 0.11, 2.02, -1.01, 2.14, 1.67, -5.09]^{\mathrm{T}} \tag{36}$$

As a result, T_a can be expressed as follows:

$$\begin{aligned} T_a &= G(T_1, T_2, T_4, T_6, T_{10}, T_{14}) \\ &= 56.80 + 0.11T_1 + 2.02T_2 - 1.01T_4 + 2.14T_6 \\ &\quad + 1.67T_{10} - 5.09T_{14} \end{aligned} \tag{37}$$

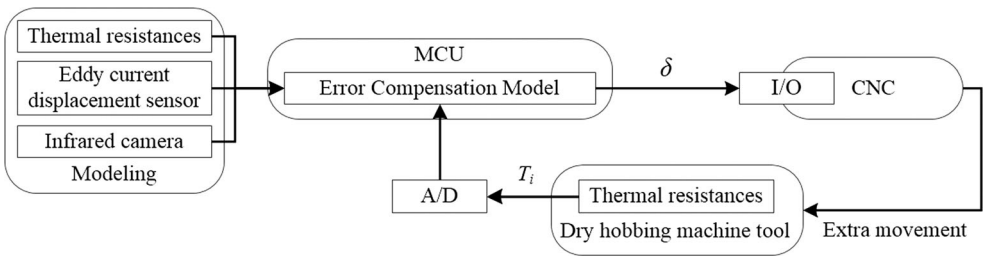

Fig. 10 Implementation of thermal error compensation

Experiments were carried out in section 5 to validate that the prediction model of T_a is effective. Substitute Eq.(37) into Eq.(21), the result is

$$\delta_T = F(G(T_1, T_2, T_4, T_6, T_{10}, T_{14})) \tag{38}$$

4.5 Thermal error modeling and implementation of compensation

As the compensation of both machine tool thermal errors and workpiece thermal deformation errors is realized by adding an extra movement to the hob spindle to change the distance of centers of hob spindle and workpiece spindle in x direction, the thermal error compensation value, δ, could be calculated using

$$\begin{aligned}\delta &= \delta_M + \delta_T \\ &= \mathrm{H}(\Delta T_1, \Delta T_2, \Delta T_4, \Delta T_{10}, \Delta T_{13}, \Delta T_{14}) \\ &\quad + F(G(T_1, T_2, T_4, T_6, T_{10}, T_{14}))\end{aligned} \tag{39}$$

Figure 10 shows the compensation procedures of thermal errors. During machining, the temperature variations of T_1, T_2, T_4, T_{10}, T_{13}, T_{14} and temperature of T_1, T_2, T_4, T_6, T_{10}, T_{14} are measured with thermal resistances, and the data are sent to the SCM. Then, the compensation model, Eq. (39), is used to calculate the compensation value, δ, in accordance with the temperature data. Finally, the compensation value is sent to the CNC of the dry hobbing machine tool, and an extra movement is added to the hob spindle to accomplish the compensation.

5 Validation

Some experiments were carried out to evaluate the performance of the compensation model. The machining parameters and the locations of sensors are same as previous case in section 3. Those experiments were carried out in summer, and the ambient temperature range from 26 to 35 °C. In those

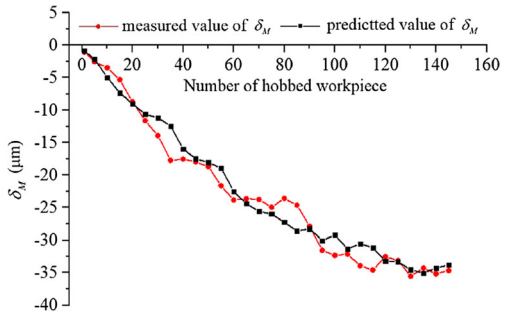

Fig. 11 Predicted value and measured value of machine tool thermal errors

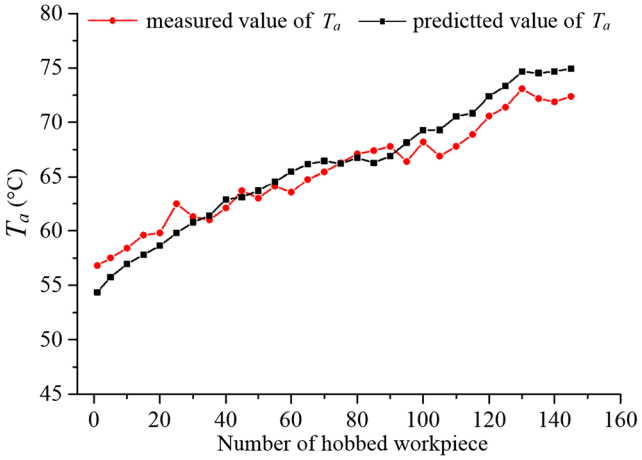

Fig. 12 Predicted value and measured value of workpiece temperature

experiments, the dry hobbing machine tool kept running for about 4 h, until 145 workpieces were processed.

Comparison between the measured value of machine tool thermal errors and the predicted value of machine tool thermal errors that calculated using machine tool error compensation model, Eq. (30), is represented in Fig. 11. It can be observed that the model predicts the machine tool thermal errors well, and the residual error range from −4 to 6 μm. Figure 12 shows the measured value of hobbed workpiece temperature and the predicted value of hobbed workpiece temperature that calculated using Eq. (37). The predicted value of hobbed workpiece temperature is fit well with measured value of hobbed workpiece temperature, and the residual error range from −2.5 to 2.4 °C, which is acceptable. It shows that the prediction model of T_a is effective.

As shown in Fig. 3, the tooth thickness errors, Δs, could be calculated by s_{y1} and s_{y3}, where s_{y1} is the tooth thickness of gear in S_1, s_{y3} is the tooth thickness of gear in S_3 on the same Y-cylinder. s_{y3} was measured by Klingelnberg Gear Measuring Center, while the hobbed workpiece was cooled to T_b. Comparison between tooth thickness errors, Δs_1, Δs_2 and Δs_3, is presented in Fig. 13. Where Δs_1 is

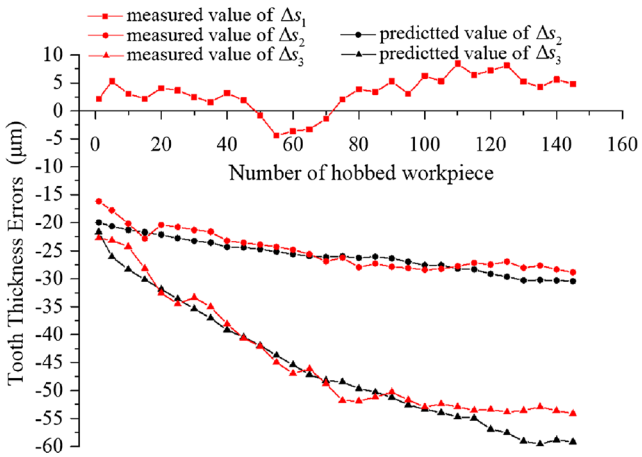

Fig. 13 Predicted values and measured values of tooth thickness errors

the tooth thickness errors of gears, which are hobbed with compensation of δ_M and δ_T. Δs_2 is the tooth thickness errors of gears, which are hobbed with compensation of δ_M. Δs_3 is the tooth thickness errors of gears, which are hobbed without compensation.

It can be observed that the measured value of Δs_2 ranges from −18 to −28 μm, and measured value of Δs_3 ranges from −22 to −59 μm. It illustrates that the workpiece thermal deformation has a great influence on tooth thickness errors. The profile deviation of hobbed workpiece is mainly caused by the factors as eccentricity of hob spindle and work table, vibration, geometric precision of hob, feed rate, et al. According to ISO 1328-1, the total profile deviation tolerance of the workpiece is 16.0 μm, on condition that the hobbed workpiece can reach precision IT7. After compensation, Δs_1 ranges from –4 to 8 μm. The workpiece that hobbed with compensation could reach the demand of next process, which demonstrates that the compensation model is effective.

6 Conclusions

In this paper, a thermal error compensation model of dry hobbing machine tool considering workpiece thermal deformation has been developed. And, an experimental system for a kind of dry hobbing machine tool is constructed to develop the compensation model. The following conclusions are drawn by this study:

(1) In dry hobbing, workpiece thermal deformation has a great influence on tooth thickness errors. The compensation of workpiece thermal deformation errors, as well as machine tool thermal errors, could be realized by adding an extra movement to the hob spindle to change the distance between centers of hob spindle and workpiece spindle in x direction.
(2) The compensation model of workpiece thermal deformation errors could be obtained by the prediction model of hobbed workpiece temperature, which is obtained using an appropriate linear combination of representative temperature variables.
(3) The fuzzy clustering method is able to find the representative temperature variables for prediction model of hobbed workpiece temperature and compensation model of machine tool thermal errors.
(4) Some verification experiments show that the proposed method can reduce tooth thickness errors that induced by both machine tool thermal deformation and workpiece thermal deformation significantly. Furthermore, this model can be applied to ordinary error compensation system conveniently.

Acknowledgments This research is supported by the National Natural Science Foundation of China (Grant No. 51475058), Program for New Century Excellent Talents in University of China (Grant No. NCET-13-0628), and National High Technology Research and Development Program of China (863 Program) (Grant No. 2012AA040107).

References

1. Claudin C, Rech J (2009) Development of a new rapid characterization method of hob's wear resistance in gear manufacturing—application to the evaluation of various cutting edge preparations in high speed dry gear hobbing. J Mater Process Technol 209(11):5152–5160. doi:10.1016/j.jmatprotec.2009.02.014
2. Bryan J (1990) International status of thermal error research. CIRP Ann Manuf Technol 39(2):645–656. doi:10.1016/S0007-8506(07)63001-7
3. Guo Q, Yang J, Wu H (2010) Application of ACO-BPN to thermal error modeling of NC machine tool. Int J Adv Manuf Technol 50(5):667–675. doi:10.1007/s00170-010-2520-y
4. Han J, Wang L, Wang H, Cheng N (2012) A new thermal error modeling method for CNC machine tools. Int J Adv Manuf Technol 62(1):205–212. doi:10.1007/s00170-011-3796-2
5. Li Y, Zhao W, Wu W, Lu B, Chen Y (2014) Thermal error modeling of the spindle based on multiple variables for the precision machine tool. Int J Adv Manuf Technol 72(9):1415–1427. doi:10.1007/s00170-014-5744-4
6. Wang S, Yang Y, Li X, Zhou J, Kang L (2013) Research on thermal deformation of large-scale computer numerical control gear hobbing machines. J Mech Sci Technol 27(5):1393–1405. doi:10.1007/s12206-013-0320-7
7. Sreejith PS, Ngoi BKA (2000) Dry machining: machining of the future. J Mater Process Technol 101(1):287–291. doi:10.1016/S0924-0136(00)00445-3
8. Li Y, Zhao W (2012) Axial thermal error compensation method for the spindle of a precision horizontal machining center. IEEE International Conference on Mechatronics and Automation pp 2319–2323. doi:10.1109/ICMA.2012.6285706
9. Yuan J, Ni J (1998) The real-time error compensation technique for CNC machining systems. Mechatronics 8(4):359–380. doi:10.1016/S0957-4158(97)00062-7
10. Wu CW, Tang CH, Chang CF, Shiao YS (2012) Thermal error compensation method for machine center. Int J Adv Manuf Technol 59(5):681–689. doi:10.1007/s00170-011-3533-x
11. Ruijun L, Wenhua Y, Zhang HH, Qifan Y (2012) The thermal error optimization models for CNC machine tools. Int J Adv Manuf Technol 63(9):1167–1176. doi:10.1007/s00170-012-3978-6
12. Yang H, Ni J (2005) Dynamic neural network modeling for nonlinear, nonstationary machine tool thermally induced error. Int J Mach Tools Manuf 45(4):455–465. doi:10.1016/j.ijmachtools.2004.09.004
13. Hao W, Hongtao Z, Qianjian G, Xiushan W, Jianguo Y (2008) Thermal error optimization modeling and real-time compensation on a CNC turning center. J Mater Process Technol 207(1):172–179. doi:10.1016/j.jmatprotec.2007.12.067
14. Wang Y, Zhang G, Moon KS, Sutherland JW (1998) Compensation for the thermal error of a multi-axis machining center. J Mater Process Technol 75(1):45–53. doi:10.1016/S0924-0136(97)00291-4

15. Ramesh R, Mannan MA, Poo AN (2000) Error compensation in machine tools—a review. Part I: geometric, cutting-force induced and fixture-dependent errors. Int J Mach Tools Manuf 40(9):1235–1256. doi:10.1016/S0890-6955(00)00009-2
16. Bachrathy D, Insperger T, Stépán G (2009) Surface properties of the machined workpiece for helical mills. Mach Sci Technol 13(2): 227–245. doi:10.1080/10910340903012167
17. Mancisidor I, Zatarain M, Munoa J, Dombovari Z (2011) Fixed boundaries receptance coupling substructure analysis for tool point dynamics prediction. Adv Mater Res 223:622–631. doi:10.4028/www.scientific.net/AMR.223.622
18. Veldhuis SC, Elbestawi MA (1995) A strategy for the compensation of errors in five-axis machining. CIRP Ann Manuf Technol 44(1):373–377. doi:10.1016/S0007-8506(07)62345-2
19. Mou J (1997) A method of using neural networks and inverse kinematics for machine tools error estimation and correction. J Manuf Sci Eng Trans ASME 119(2):247–254. doi:10.1115/1.2831101
20. Abukhshim NA, Mativenga PT, Sheikh MA (2006) Heat generation and temperature prediction in metal cutting: a review and implications for high speed machining. Int J Mach Tools Manuf 46(7): 782–800. doi:10.1016/j.ijmachtools.2005.07.024